# Shared Control of Elbow Movements with Functional Electrical Stimulation and Exoskeleton Assistance

Nathan Dunkelberger<sup>1</sup>, Skye A. Carlson<sup>2</sup>, Jeffrey Berning<sup>1</sup>, Kyra C. Stovicek<sup>2</sup>, Eric M. Schearer<sup>2</sup>, and Marcia K. O'Malley<sup>1</sup>

Abstract—Individuals who suffer from paralysis as a result of a spinal cord injury list restoration of arm and hand function as a top priority. FES helps restore movement using the user's own muscles, but does not produce accurate and repeatable movements necessary for many functional tasks. Robots can assist users in achieving accurate and repeatable movements, but often require bulky hardware to generate the necessary torques. We propose sharing torque requirements between a robot and FES to reduce robot torque output compared to a robot acting alone, yet maintain high accuracy. Cooperative PD and model predictive control algorithms were designed to share the control between these two torque sources. Corresponding PD and MPC algorithms that do not use FES were also designed. The control algorithms were tested with 10 able-bodied subjects. Torque and position tracking accuracy were compared when the system was commanded to follow a functional elbow flexion/extension trajectory. The robot torque required to achieve these movements was reduced for the shared control cases compared to the algorithms acting without FES. We observed a reduction in position accuracy with the MPC shared controller compared to the PD shared controller, while the MPC shared controller resulted in greater reductions in torque requirements. Both of these shared algorithms showed improvements over existing options, and can be used on any given trajectory, allowing for better transferability to functional

#### I. INTRODUCTION

Restoration of arm and hand function is a top priority among people with tetraplegia due to cervical spinal cord injuries (SCI) [1]. With scarce rehabilitation and assistive technology options, these individuals are largely dependent on full-time caregivers for feeding, grooming, and many other activities of daily living.

Functional electrical stimulation (FES) is a promising assistive technology to restore arm and hand function because it activates a person's own paralyzed muscles, resulting in very low energy consumption and high embodiment of an FES system. However, FES cannot produce sufficient torques to enable whole-arm reaching movements in people with tetraplegia, as many muscles are unresponsive to FES [2], [3]. Further, multi-joint motions are notoriously hard to control with FES even with the most advanced systems [4].

\*This material is based upon work supported by the National Science Foundation under Grant Nos. CBET 2025130 and 2025142.

Augmenting FES with an assistive robot offers additional torque to support whole arm reaching while also offering improved movement accuracy, but this comes at the expense of increased bulkiness and decreased wearability of the combined FES-robotic system. An optimal combination of FES and an assistive robot would maximize the contribution of FES to minimize size and power requirements of the robot.

Previous work has explored using FES in combination with robotic devices, but to date, these approaches have not truly combined and coordinated the actuation strategies for upper limb movements [5]. Instead, each of the actuation types has been used to achieve separate functions. Robotic devices have been used to lock degrees of freedom [6], [7] or as gravity compensation [8] enabling the muscles to relax and preventing fatigue. Other work used robotic support devices to actuate one set of degrees of freedom, while FES was used to actuate another set [4], [9], [10]. Typically the robot controls motions that need precision, such as elbow flexion and extension, while FES is used for coarse movements, such as grasping. For motions with coupled degrees of freedom, such as shoulder, elbow, and wrist movements, these strategies pit FES against a robot-imposed locked-joint, gravity, or single-joint motion constraint, essentially wasting the free actuation from FES and transferring it to the robot. In lower limbs, more advanced cooperative control algorithms have been explored, largely enabled by the repetitive motion of gait [11], [12], [13]. Goal-directed reaching movements with the upper limb are much more diverse than gait and are not periodic in nature.

A truly shared control approach for hybrid FES and robotic control of upper limb reaching movements is needed to realize general movement assistance rather than specific movement profiles. Successful integration requires that each system is aware of the expected contributions of the other during coordinated tasks. Recent work is starting to move in this direction, with model-based algorithms being used to power FES in combination with gravity compensation from a robot [14]. In this paper, we demonstrate shared control of elbow flexion and extension movements with FES and exoskeleton assistance acting in coordination to follow a desired trajectory. Further, we show that a model-based controller for the exoskeleton, which has knowledge of the expected contributions of FES, requires significantly less robot torque than a standard PD control algorithm, with minimal loss in trajectory following accuracy.

N. Dunkelberger, J. Berning, and M. K. O'Malley represent the Mechatronics and Haptic Interfaces Lab, Department of Mechanical Engineering, Rice University, Houston, TX, 77005. {nbd2, jb139, omalleym}@rice.edu

S. A. Carlson, K. C. Stovicek, and E. M. Schearer represent the Center for Human-Machine SystemsCombined, Cleveland State University, Cleveland, OH, 44115. {s.a.carlson, k.c.stovicek}@vikes.csuohio.edu, e.schearer@csuohio.edu

#### II. METHODS

We developed two shared control algorithms, one based on proportional-derivative control and one using model predictive control, to achieve a functional elbow flexion movement using a combination of FES and a rigid exoskeleton robot. Data were gathered from ten able bodied participants with the right arm following a functional elbow flexion trajectory.

#### A. Control Strategies

1) Proportional Derivative Control: We implemented a proportional derivative (PD) controller for torque due to the exoskeleton, and a proportional controller for torque due to FES. The FES control was limited to a proportional controller because the physiological time-delay due to FES can cause oscillatory motion if derivative action is implemented. The PD control law is shown in (1) and (2),

$$\tau_{exo} = K_{p\_exo}(\theta - \theta_d) - K_{d\_exo}\dot{\theta} \tag{1}$$

$$\tau_{fes} = K_{p-fes}(\theta - \theta_d) \tag{2}$$

where  $\theta_d$  is the desired position and  $K_{p-fes}$  describes how much torque effort can be provided due to  $\tau_{fes}$ . In this controller,  $K_{p,fes}$  is also inherently limited due to the physiological delay between when FES is commanded, and when torque is output [15].

The gains  $K_{p\_exo}$  and  $K_{d\_exo}$  were empirically chosen to effectively track functional trajectories for a humanexoskeleton combined system while avoiding oscillatory motion. The value of  $K_{p-fes}$  was determined in pilot testing to ensure that the control does not result in oscillations, but still provides some assistive torque. For the version of the control strategy that does not include FES,  $\tau_{fes} = 0$ .

2) Model Predictive Control: A model predictive control (MPC) algorithm was used to share the torque between the exoskeleton and the FES. To use MPC, we first need to describe the dynamic model. The system of interest in this formulation is the combined system of the exoskeleton and the participant's arm, which can be seen in Fig. 1. For this model, we assume that the masses and inertias of the exoskeleton and the arm can be combined into one lumped model, and that they move together as a rigid body.

The state variables for this control problem are the position and velocity of the elbow flexion extension joint, defined as  $\theta$  and  $\theta$ , respectively.  $\theta$  is measurable from an encoder on the motor, and a filtered estimate for  $\dot{\theta}$  is provided from the data acquisition device. The inputs to the system include the torque provided to the elbow flexion extension joint of the exoskeleton,  $\tau_{exo}$ , and the torque due to FES,  $\tau_{fes}$ , which includes torque from the biceps and the triceps. The dynamic system is then defined as follows,

$$\tau_{fes} + \tau_{exo} = J\ddot{\theta} + F_k \tanh(10\dot{\theta}) + F_C\dot{\theta} + mgl\sin(\theta + \theta_{eq})$$
(3)

where J is the inertia of the combined exoskeleton-arm system, m is the mass of the combined system,  $F_k$  is the kinetic friction,  $F_c$  is viscous friction, l is the distance to the center of mass of the combined system, and  $\theta_{eq}$  is

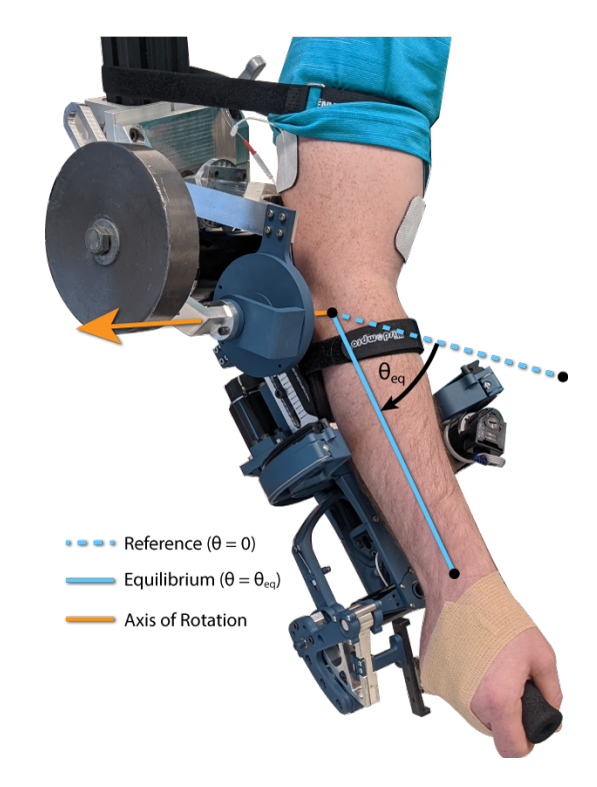


Fig. 1. The MAHI Open Exo shown with a participant in the reference position (elbow joint at a right angle,  $\theta = 0$ ). The equilibrium position,  $\theta_{eq}$ , is where the user's arm naturally rests when there is no torque provided. All joints except the elbow flexion/extension joint are controlled to hold a neutral position for the duration of the experimental protocol.

the equilibrium position of the combined system. For this experiment, the friction in the arm was considered to be negligible compared to the friction in the exoskeleton, which was characterized in previous work [16].

The inertia J is calculated according to the positioning of subject-specific adjustable parameters, and includes an estimated inertia of the arm. The inertia of the arm is calculated as if it were a cylinder with the radius based on the participant's measured forearm circumference and a mass of 2 kg, which was empirically found to provide suitable tracking for most participants. The term mgl was replaced by a single term, M, and M and  $\theta_{eq}$  were determined for each subject by performing a nonlinear curve fit of (4) by using the steady state torques required to keep the arm and exoskeleton in several positions throughout the workspace.

$$\tau_{exo} = M\sin(\theta + \theta_{eq}) \tag{4}$$

The formulation of the MPC problem was defined with the following state, x, output, y, and input, u. Because the data acquisition device provides both the position and a filtered estimate of the velocity, C is the identity matrix.

$$x = [q, \dot{q}]^T \tag{5}$$

$$C = \mathbb{I}_2 \tag{6}$$

$$y = Cx \tag{7}$$

$$y = Cx$$

$$u = [\tau_{exo}, \tau_{fes}]^{T}$$
(8)

In the model predictive control problem, discrete timesteps,

i are spaced out at an interval of  $T_s$ . A linearized version of the dynamics about an operating time, k, can be calculated at time  $i \ge k$  using the state at time k,  $x_k$ , and input at time k,  $u_k$ , using the following equations.

$$A = \frac{\partial \dot{x}}{\partial x} \tag{9}$$

$$B = \frac{\partial \dot{x}}{\partial u} \tag{10}$$

$$\dot{x}_i = A|_{x=x_k} x_i + B|_{x=x_k} u_i + \dot{x}|_{x=x_k, u=u_k}$$
 (11)

In the MPC formulation, the current state and input are provided, and a cost function is minimized to provide an optimal input over the prediction horizon, N. The cost function weights several parameters that are important to this control problem, including the state error,  $y_i - r_i$  where  $r_i$  is the desired state at time i, the integral of position error,  $e_i$ , the magnitude of the torques,  $u_i$ , and the change in torques,  $\Delta u_i = u_i - u_{i-1}$ . This resulting cost function evaluated at time step i is shown below,

$$J_i = (y_i - r_i)^T Q(y_i - r_i) + e_i^T P e_i$$
  
 
$$+ u_i^T R_m u_i + \Delta u_i^T R \Delta u_i$$
 (12)

where  $Q \in \mathbb{R}^{2 \times 2}$ ,  $P \in \mathbb{R}^{1 \times 1}$ ,  $R_m \in \mathbb{R}^{2 \times 2}$ , and  $R \in \mathbb{R}^{2 \times 2}$  are positive definite and diagonal weighting matrices.

The cost on state error encourages the system to follow the desired trajectory. The cost on the integral of position error places more emphasis on accurate trajectory following if it has been inaccurate for a significant amount of time. The integral term is defined as

$$e_i = \lambda e_{i-1} + T_s(y_i - r_i) \tag{13}$$

where  $0 < \lambda < 1$ , is a forgetting factor that places more emphasis on recent errors [17].

In (12), the cost of the two torque inputs of u is determined using  $R_m$ , allowing FES torque to be preferred by setting  $R_{m.exo} >> R_{m.fes}$  in (14).

$$R_m = \begin{bmatrix} R_{m\_exo} & 0\\ 0 & R_{m\_fes} \end{bmatrix} \tag{14}$$

The cost due to the change in torque,  $\Delta u$ , due to the exoskeleton and FES, is determined using R. This parameter is used to encourage the FES, which has a significant time delay, to provide gross torque in a specific direction, while the exoskeleton, which has a very small time delay, can fine tune the motions quickly. This is achieved by setting  $R_{exo} << R_{fes}$  in (15).

$$R = \begin{bmatrix} R_{exo} & 0\\ 0 & R_{fes} \end{bmatrix} \tag{15}$$

To ensure a fair comparison in torque outputs, it was necessary to achieve similar position accuracy in the case where FES was used and the case where FES was not used. To accomplish this, in the control case with FES, the weights of  $R_m$  were modified in real-time to prefer the exoskeleton if the position diverged too far from the desired trajectory.

The cost function defined in (12) is minimized as follows,

$$\underset{u(\cdot)}{\operatorname{argmin}} J = \sum_{i=1}^{N-1} J_{k+i} \tag{16}$$

subject to 
$$R(\theta_k)_{triceps} \leq \tau_{fes} \leq R(\theta_k)_{biceps},$$
 
$$\bar{y}_{k+i+1} = \bar{y}_{k+i} + T_s \dot{\bar{x}}_{k+i}$$

where  $R(\theta_k)_{triceps}$  and  $R(\theta_k)_{biceps}$  are the minimum and maximum torque available from the triceps and biceps, respectively, given the current configuration,  $\theta_k$ , as in (17).

A multiple shooting optimal control problem was created to minimize (16) using the C++ based optimal control framework, CasADi [18]. A compiled version of the control problem was loaded at runtime, and solved using the nonlinear solver, IPOPT [19]. When the optimal control input was found, the result,  $u(\cdot)$ , was used as control inputs to the exoskeleton and FES until another optimization step finished.

For the version of this controller that does not use FES,  $R_{m.exo} = 0$ , which prefers to use all torque from the robot. 3) FES command: For either control case, once the desired torque was calculated, the desired muscle activations,  $\alpha \in \mathbb{R}^{2\times 1}$ , were calculated from the following equation,

$$R(\theta_k)\alpha = \tau_{fes} \tag{17}$$

where  $\theta_k$  corresponds to the position of the upper-limb,  $R(\theta_k) \in \mathbb{R}^{1 \times 2}$  corresponds to the learned mapping between the max torque output of each joint and the position of the upper-limb [20], and  $\alpha$  consists of terms that all lie between 0 and 1.

Because in the general case there are more FES control inputs than movable degrees of freedom, there can be several solutions to this problem. To find a realtime solution, we use a quasi-newton algorithm to minimize a cost function,  $J_{fes}$ , that we specify as follows [20].

$$J_{fes} = c_1 \alpha^2 + c_2 ||R(\theta_k)\alpha - \tau_{fes}||^2 + c_3 K$$
 (18)

$$K = \sum_{i=1}^{2} k_i \tag{19}$$

$$k_i = \begin{cases} \alpha_i^2 & \alpha_i < 0\\ 0 & 0 \le \alpha_i \le 1\\ (1 - \alpha_i)^2 & \alpha_i > 1 \end{cases}$$
 (20)

In this case, the first term of the cost function penalizes the use of higher amounts of activation, the second term penalizes incorrectly provided torque, and the third term penalizes unusable activations, with  $c_1$ ,  $c_2$ , and  $c_3$  indicating weightings on each of these terms, respectively.

## B. Participants

Ten able-bodied subjects (6 male, 4 female, average age 24) participated in the experiment and provided informed consent. The participants did not have physical or cognitive impairments that could have interfered with the study. Most of them had little to no experience with electrodes placed on their muscles. The study was approved by the institutional review boards at Rice University (IRB #FY2017-461) and Cleveland State University (IRB #30213-SCH-HS).

### C. Experimental Protocol

The MAHI Open Exo (MOE) was used as the upper-limb exoskeleton in these experiments [16]. The participant was seated in a chair and asked to place their right arm in MOE. The height, forearm length, and counterweight of the exoskeleton were adjusted to ensure that the arm began in a neutral resting position, setting  $\theta_{eq}$  to approximately  $-40^{\circ}$ , and aligning the remaining joints of the arm to the exoskeletons degrees of freedom (DOF), as shown in Fig. 1.

Once the exoskeleton was adjusted, the transdermic electrical stimulation system [21] electrodes (2 inch square) could be placed on the participant to deliver FES to the biceps and triceps. To determine the most effective placement of the electrodes, a motor point pen (Compex) was used to find the muscle motor points. This process involved placing one surface electrode over the reference point while using the motor point pen to probe the surface area of the target muscle, one muscle group at a time. After the motor point was found using the motor point pen, a surface electrode was placed on the identified location. Once the electrodes were placed, the participant's arm was fitted into the exoskeleton as shown in Fig. 1, and straps were placed around the users hand, forearm, and shoulder to limit compensatory motions during stimulation.

- 1) Recruitment Curve Calibration: Stimulation amplitudes were chosen for each participant based on comfort level for expected ranges of pulsewidths (PWs). The recruitment curve calibration was then used to determine the required stimulation PW to achieve a desired level of muscle activation. The participant's minimum PW value that provided a measurable torque, as well as the maximum value that was comfortable were recorded. Recruitment curves were then found using the deconvolved ramp method [22].
- 2) Gaussian Process Regression (GPR) Calibration: As FES stimulates a muscle, the configuration of the arm impacts the possible torque output. To model this mapping, a Gaussian Process Regression (GPR) model was created to identify the torque output at maximum stimulation ( $\alpha = 1$ ), given the configuration,  $\theta_k$  as in [20].

To record these data, the combined exoskeleton and arm system was moved to eight elbow positions equally spaced between -65° and +20°, three times each. At each position, the exoskeleton remained stationary while the biceps and triceps were independently stimulated at their maximum PW. The torque required for the exoskeleton to maintain its position was recorded.

3) Study: A series of 20 trials was performed where the combined exoskeleton and arm system followed a trajectory based on a functional task of individuals moving a cup to various locations [23]. There were 5 trials for each of the 4 conditions; PD without FES, PD with FES, MPC without FES, MPC with FES. The trials were randomized to avoid bias in the results. After 10 trials, the participant was allowed to rest for several minutes to limit fatigue in the biceps and triceps. The participants were asked to remain relaxed throughout the study.

#### D. Data Analysis

Means of squared torques for each control case were calculated for each participant as an average across the five trials for that case. RMS position error with respect to the desired trajectory was also calculated for each individual participant for each condition.

To understand how these novel control algorithms compare to a standard PD control without FES, the mean of squared torques were normalized to that of PD control without FES. This is useful because the baseline power required to move the combined human-exoskeleton system varied from participant to participant because of the differing arm sizes between participants.

To determine if there was a difference between the non-normalized required power output across the four different control conditions, a repeated measures analysis of variance (ANOVA) was used with the dependent variable of non-normalized mean of squared torques, and within-subject independent variables of control algorithm (PD or MPC) and FES (with or without). The ANOVA was followed by pairwise t-tests with Bonferroni corrections, which results at a statistically significant p < 0.0125. Another repeated measures ANOVA, followed by pairwise t-tests with Bonferroni corrections, was used to determine if there was a difference between the same cases for RMS position error.

#### III. RESULTS

We compared the performance in tracking a functional elbow flexion extension trajectory with two controllers, PD and MPC, each in cases with and without FES assistance. Two primary outcome measures are used in the comparison. The mean of squared torques serves as a measure of electrical power consumption of the motor, which is related to the amount of on-board power that a user might need in a wearable assistive device. The RMS position error serves as a representation of trajectory following accuracy of the controller during completion of a functional task.

There was a decrease in mean of squared torque in both MPC and PD control cases when FES was used compared to when FES was not used. As shown in Table I, in the PD case, the mean of squared torque was decreased by  $0.596 \, \mathrm{Nm^2} \ (p = 0.007^*)$ , and in the MPC case, the mean of squared torque was decreased by  $1.019 \, \mathrm{Nm^2} \ (p = <0.001^*)$ . When comparing just the cases with FES, we find that the MPC case has a significantly smaller mean of squared torques  $(p = 0.006^*)$ . The torques used throughout the functional trajectory, averaged across participants, can be visualized in each of these cases in the bottom row of Fig. 2.

Normalizing the mean of squared torques to the case of PD control without FES, we see that participants saw an average of 32.1% reduction in mean of squared torque in the MPC with FES case whereas the subjects saw an average of 19.6% reduction of torque in the PD with FES case. These results are shown in Fig. 3, with  $\pm$  1 standard error of mean (SEM) shown as error bars. In this graph, the PD without FES case is provided as a reference, but is necessarily 1.0 in all cases because it is the value normalized against.

Summary of results for mean of squared torque and RMS error, averaged across subjects, with SEM shown in parenthesis. Differences between the means and P-values for paired t-tests are also shown. \*p < .0125 due to Bonferonni correction.

Metric	Control	without FES	with FES	diff	p-value
Mean Squared	PD	2.710 (0.476)	2.114 (0.362)	-0.596 $-1.019$	0.007*
Torque (Nm <sup>2</sup> )	MPC	2.803 (0.459)	1.784 (0.298)		< 0.001*
RMS Error	PD	1.108 (0.066)	1.004 (0.054)	-0.104 +0.926	0.006*
(Degrees)	MPC	1.561 (0.255)	2.487 (0.322)		0.006*

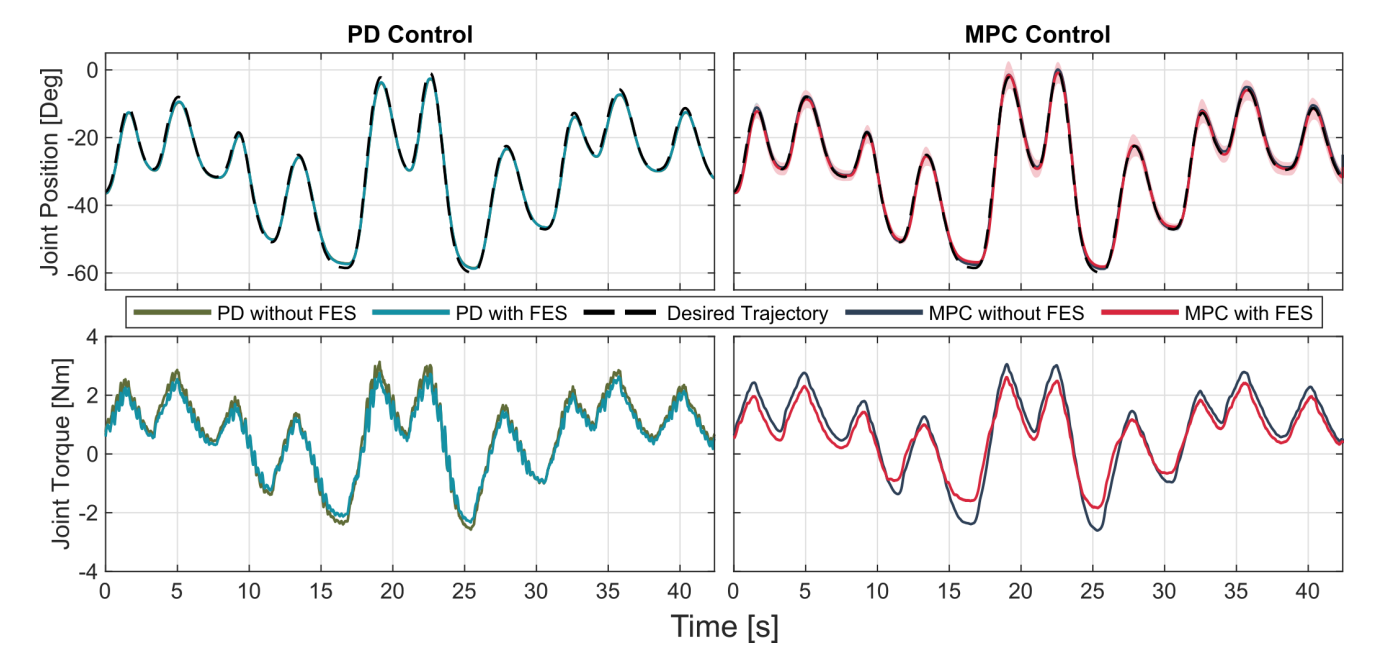


Fig. 2. Plots of position (top) and torque (bottom) averaged between subjects over the functional movement trajectory. The position plots show the mean in solid colors with  $\pm 1$  standard deviation shaded around the trajectory.

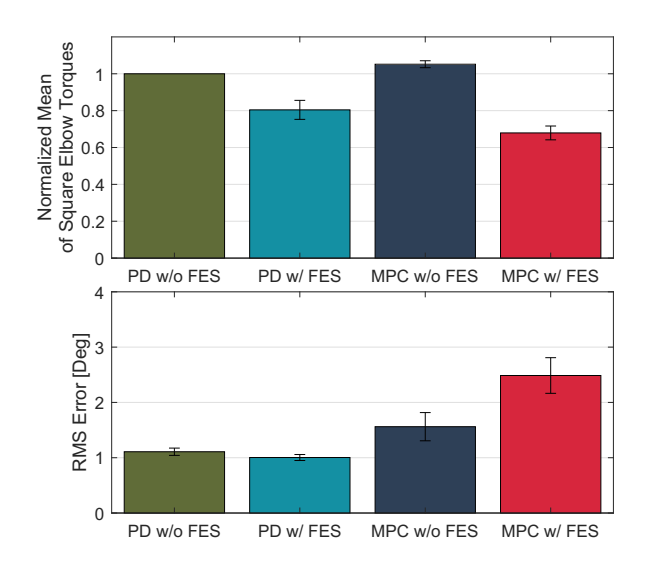


Fig. 3. The top graph shows a bar chart showing the mean of squared elbow torques for each control case, normalized within subjects to the PD without FES case, with SEM shown on error bars. The bottom graph shows a bar chart of RMS error when tracking the desired trajectory for each of the control cases with SEM shown on error bars.

Quantifying accuracy, in the PD case, the RMS error was

decreased by 0.104 degrees (p=0.006\*) in the case with FES compared to the case without FES, and in the MPC case, the RMS error was increased by 0.926 degrees (p=0.006\*) in the case with FES compared to the case without FES. Comparing just the cases with FES, the MPC controller also has a higher RMS error compared to the PD controller (p=0.002\*). These mean RMS error values are shown in the bottom of Fig. 3 with  $\pm$  1 SEM shown on the error bars. The mean timeseries of elbow position is shown in the top row of Fig. 2, along with shading showing  $\pm$  1 standard deviation. The desired trajectory is also shown for reference.

#### IV. DISCUSSION

Two algorithms were presented which can be used to provide movement assistance given an input tracking goal. Because these algorithms work on any provided trajectory, rather than one specifically programmed motion, they can be applied to many functional scenarios, as long as a desired trajectory or endpoint can be provided. This is a significant advancement over many FES systems used for functional tasks that require task-specific construction of stimulation profiles by a therapist.

In completing the functional movement, both control implementations with FES saw a statistically significant reduction in mean of squared torques required by the exoskeleton to perform the movement compared to the version of those algorithms without FES. This means that less power would be consumed for the same motion profile, which could translate to more portable systems with smaller battery packs in future wearable exoskeleton designs.

Only comparing controllers that use FES, the MPC case had a larger reduction of normalized mean of squared torques compared to the PD case (32.1% compared to 19.6%), as can be see in the top of Fig. 3, showing that it could lead to more savings in power consumption. As mentioned in Section II-A, the PD with FES controller is largely limited by the physiological time delay inherent when using FES, meaning that there is a limited benefit that can be gained before resulting in oscillatory behavior. These results incentivize the use of model-based control algorithms for combining FES with robots where we can use knowledge of both sets of torque inputs to provide greater reductions in power consumption.

The MPC case with FES did show a statistically significant worse accuracy compared to the PD case with FES, with RMS errors of 1.00 and 2.49 degrees respectively. This is expected because our model of FES adds another level of uncertainty to the control method. Even with this increase, the mean RMS error was only 2.49 degrees, or 4.15% of the workspace, which is acceptable for many functional tasks. As can be seen in the position graphs in Fig. 2, the trajectories in all control conditions follow the desired trajectory very closely, with most of the large errors occurring at the extremes of the workspace.

## V. CONCLUSION

Two novel control algorithms were developed to share the torque load between FES and a robotic exoskeleton. Both control algorithms showed a reduction in power consumption compared to the robot alone case. The accuracy of the combined human-arm system was decreased in cases with MPC, but is still relatively accurate compared to what FES alone can achieve. Further, these algorithms can be applied to general movement scenarios, rather than tuning control performance for specific movements.

#### REFERENCES

- K. D. Anderson, "Targeting recovery: Priorities of the spinal cordinjured population," *Journal of Neurotrauma*, vol. 21, no. 10, pp. 1371–1383, 2004.
- [2] M. Mulcahey, B. Smith, and R. Betz, "Evaluation of the lower motor neuron integrity of upper extremity muscles in high level spinal cord injury," *Spinal Cord*, vol. 37, no. 8, p. 585, 1999.
- [3] P. Peckham, J. Mortimer, and E. Marsolais, "Upper and lower motor neuron lesions in the upper extremity muscles of tetraplegics," *Spinal Cord*, vol. 14, no. 2, pp. 115–121, 1976.
- [4] A. B. Ajiboye, F. R. Willett, D. R. Young, W. D. Memberg, B. A. Murphy, J. P. Miller, B. L. Walter, J. A. Sweet, H. A. Hoyen, M. W. Keith *et al.*, "Restoration of reaching and grasping movements through brain-controlled muscle stimulation in a person with tetraplegia: a proof-of-concept demonstration," *The Lancet*, vol. 389, no. 10081, pp. 1821–1830, 2017.
- [5] N. Dunkelberger, E. M. Schearer, and M. K. O'Malley, "A review of methods for achieving upper limb movement following spinal cord injury through hybrid muscle stimulation and robotic assistance," *Experimental Neurology*, p. 113274, 2020.

- [6] C. Klauer, T. Schauer, W. Reichenfelser, J. Karner, S. Zwicker, M. Gandolla, E. Ambrosini, S. Ferrante, M. Hack, A. Jedlitschka, A. Duschau-Wicke, M. Gföhler, and A. Pedrocchi, "Feedback control of arm movements using neuro-muscular electrical stimulation (nmes) combined with a lockable, passive exoskeleton for gravity compensation," Frontiers in Neuroscience, vol. 8, no. 262, pp. 1–16, 2014.
- [7] E. Ambrosini, S. Ferrante, J. Zajc, M. Bulgheroni, W. Baccinelli, E. D'Amico, T. Schauer, C. Wiesener, M. Russold, M. Gfoehler, M. Puchinger, M. Weber, S. Becker, K. Krakow, M. Rossini, D. Proserpio, G. Gasperini, F. Molteni, G. Ferrigno, and A. Pedrocchi, "The combined action of a passive exoskeleton and an EMG-controlled neuroprosthesis for upper limb stroke rehabilitation: First results of the RETRAINER project," *IEEE International Conference on Rehabilitation Robotics*, pp. 56–61, 2017.
- [8] G. Cannella, D. S. Laila, and C. T. Freeman, Design of a Hybrid Adaptive Support Device for FES Upper Limb Stroke Rehabilitation, 01 2016, vol. 38, pp. 13–22.
- [9] S. Schulz, S. B, W. R, C. Pylatiuk, and M. Reischl, "The hybrid fluidic driven upper limb orthosis - orthojacket," *Proceedings of the 2011 MyoElectric Controls/Powered Prosthetics Symposium Fredericton*, 08 2011.
- [10] R. Varoto, E. S. Barbarini, and A. Cliquet, "A hybrid system for upper limb movement restoration in quadriplegics," *Artificial Organs*, vol. 32, no. 9, pp. 725–729, 2008.
- [11] K. H. Ha, S. A. Murray, and M. Goldfarb, "An approach for the cooperative control of fes with a powered exoskeleton during level walking for persons with paraplegia," *IEEE Transactions on Neural Systems and Rehabilitation Engineering*, vol. 24, no. 4, pp. 455–466, 2016.
- [12] T. C. Bulea, R. Kobetic, M. L. Audu, J. R. Schnellenberger, G. Pinault, and R. J. Triolo, "Forward stair descent with hybrid neuroprosthesis after paralysis: Single case study demonstrating feasibility," *Journal of Rehabilitation Research and Development*, vol. 51, no. 7, p. 1077, 2014.
- [13] A. J. del Ama, A. Gil-Agudo, J. L. Pons, and J. C. Moreno, "Hybrid FES-robot cooperative control of ambulatory gait rehabilitation exoskeleton," *Journal of Neuroengineering and Rehabilitation*, vol. 11, no. 1, pp. 1–15, 2014.
- [14] D. Wolf and E. Schearer, "Trajectory optimization and model predictive control for functional electrical stimulation-controlled reaching," IEEE Robotics and Automation Letters, 2022.
- [15] C. L. Lynch and M. R. Popovic, "Functional electrical stimulation," IEEE Control Systems Magazine, vol. 28, no. 2, pp. 40–50, Apr 2008.
- [16] N. Dunkelberger, J. Berning, K. J. Dix, S. A. Ramirez, and M. K. O'Malley, "Design, characterization, and simulation of the mahi open exoskeleton upper limb robot (in review)," *IEEE/ASME International Conference on Advanced Intelligent Mechatronics*, 2022.
- [17] G. P. Incremona, M. Messori, C. Toffanin, C. Cobelli, and L. Magni, "Model predictive control with integral action for artificial pancreas," *Control Engineering Practice*, vol. 77, pp. 86–94, 2018.
- [18] J. A. E. Andersson, J. Gillis, G. Horn, J. B. Rawlings, and M. Diehl, "CasADi – A software framework for nonlinear optimization and optimal control," *Mathematical Programming Computation*, vol. 11, no. 1, pp. 1–36, 2019.
- [19] A. Wächter and L. T. Biegler, "On the implementation of an interior-point filter line-search algorithm for large-scale nonlinear programming," *Mathematical Programming*, vol. 106, no. 1, pp. 25–57, Mar 2006.
- [20] D. N. Wolf, Z. A. Hall, and E. M. Schearer, "Model learning for control of a paralyzed human arm with functional electrical stimulation," in 2020 IEEE International Conference on Robotics and Automation (ICRA). IEEE, 2020, pp. 10148–10154.
- [21] S. Trier, J. Buckett, A. Campean, M. Miller, F. Montague, T. Vrabec, and J. Weisgarber, "A modular external control unit for functional electrical stimulation," 01 2001.
- [22] W. Durfee and K. MacLean, "Methods for estimating isometric recruitment curves of electrically stimulated muscle," *IEEE Transactions on Biomedical Engineering*, vol. 36, no. 7, pp. 654–667, 1989.
- [23] A. M. Valevicius, Q. A. Boser, E. B. Lavoie, C. S. Chapman, P. M. Pilarski, J. S. Hebert, and A. H. Vette, "Characterization of normative angular joint kinematics during two functional upper limb tasks," *Gait Posture*, vol. 69, pp. 176–186, 03 2019.